

# *B* Production and Oscillations at DELPHI

Gary Barker

University of Karlsruhe, Germany

Received: 9 October 2003 / Accepted: 15 October 2003 /

Published Online: 8 April 2004 – © Springer-Verlag / Società Italiana di Fisica 2004

**Abstract.** New, preliminary, results from DELPHI are presented covering a first measurement of the  $B_u^+$ -meson branching fraction, updates to  $B_s^0$  oscillation analyses using high  $p_t$  leptons and  $D_s$ -lepton correlations and studies of the orbitally excited states,  $B_{u,d}^{**}, B_s^{**}$ .

## 1 Introduction

We report on the latest updates to analyses from DELPHI in the areas of  $b$ -hadron production fractions,  $B_s^0$  oscillations and  $B^{**}$  production.

## 2 A first measurement of $f_{B_u}, f_{B_d}$

The production fractions of the *weakly* decaying states  $B_u^+, B_d^0$  are defined as,

$$f_{B_u} = \text{BR}(\bar{b} \rightarrow B^+) = \text{BR}(b \rightarrow B^-)$$
$$f_{B_d} = \text{BR}(\bar{b} \rightarrow B^0) = \text{BR}(b \rightarrow \bar{B}^0).$$

Because of the strong decays of orbitally excited ( $L = 1$ )  $B$ -mesons, generically known as  $B^{**}$  states, these fractions are not expected to be numerically the same as the fractions seen directly after the fragmentation process. However, the equality  $f_{B_u} = f_{B_d}$  is expected to still hold.

Precise knowledge of  $f_{B_u}, f_{B_d}$  is desirable since they are an important input and systematic error for many analyses e.g.  $B^0 - \bar{B}^0$  oscillations and in studies of the CKM triangle parameters. In addition they give valuable information concerning the start of the fragmentation process due to the fact that  $b$ -quarks are produced, to first order, only from the  $Z^0$  decay and not from some secondary process.

This analysis represents a first direct measurement of  $f_{B_u}, f_{B_d}$ . Indirect determinations of the fractions are currently made by the Heavy Flavour Averaging Group by combining all available information on  $f_{B_s}$  and  $f_{b\text{-baryon}}$  from LEP and CDF and by imposing the constraints  $f_{B_u} = f_{B_d}$  and  $f_{B_u} + f_{B_d} + f_{B_s} + f_{b\text{-baryon}} = 1$ . Full details of the analysis can be found in [1].

### 2.1 Experimental method and results

The method reconstructs the charge of weakly decaying states by reconstructing, for each charged particle in a

hemisphere, the probability  $P_B$  that it originates from a  $b$ -hadron decay rather than from fragmentation. For this, neural network techniques were used with the following input variables: the probability that the particle fits to the primary vertex, the momentum, the rapidity of the particle with respect to the thrust axis and the reconstructed flight distance from the primary to the secondary vertex and the error. The charge of the weakly decaying state was then constructed through,

$$Q_B = \sum_{i=1}^N Q_i P_{B,i}$$

where  $N$  is the number of accepted particles in the hemisphere and  $Q_i$  is the reconstructed particle charge. After a  $b$ -tag cut in the opposite hemisphere that leaves 2% background, a fit was made to the (background subtracted)  $Q_B$  distribution reconstructed from data taken in 1994 and 1995 using the following function,

$$\left( f_{X_B^+} \cdot Q_{X_B^+} + f_{X_B^0} \cdot Q_{X_B^0} \right)$$

where  $X_B^+$  and  $X_B^0$  indicates any charged and neutral  $b$ -hadron respectively. The  $Q$  distributions were taken from simulation and the constraint,  $(f_{X_B^+} + f_{X_B^0}) = 1$ , was imposed. Figure 1 shows the result of the fit together with the simulated neutral and charged distributions. The analysis was able to control the level of uncertainty that is introduced by taking the fit function shapes from simulation, by a self-calibration method based on events where both hemispheres contain a  $Q_B$  tag. The result of the fit was,  $f^+ = 42.09 \pm 0.82(\text{stat.}) \pm 0.89(\text{syst.})\%$ , where the systematic error is dominated by the  $Q_B$  self calibration procedure. The quantity of interest,  $f_{B_u}$ , then follows by subtracting off contributions from charged-strange baryons,  $f_{\Xi_b^-} = 1.1 \pm 0.5\%$  [2] (it is assumed that the  $\Omega_b$  rate is negligible), to give the final result

$$f_{B_u} = 40.99 \pm 0.82(\text{stat.}) \pm 1.11(\text{syst.})\%.$$

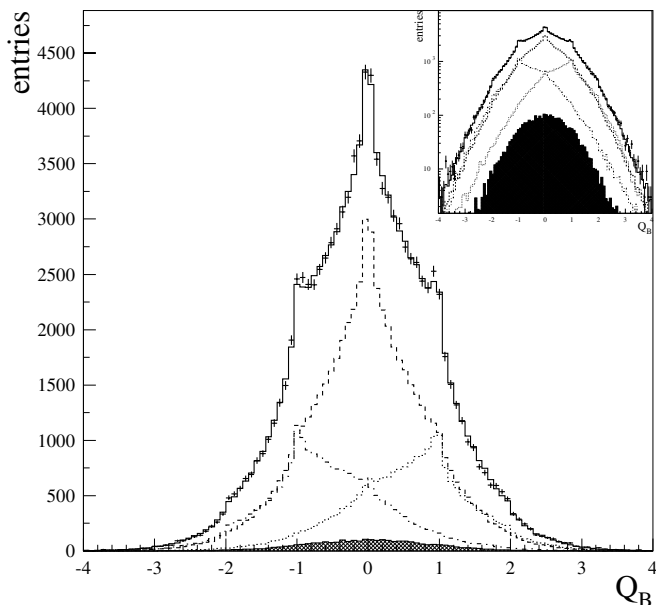


**Fig. 1.** The  $Q_B$  distribution for data (points) with the result of the fit superimposed (solid histogram) on both a linear and log scale (insert). The distributions for neutral (dashed histogram), negatively (dashed-dotted histogram) and positively (dotted histogram) charged  $b$ -hadrons are also shown.

### 3 $B_s^0$ oscillations update

DELPHI has recently updated two previously published results on  $B_s^0$  oscillations with the following improvements:

- **High  $p_t$  lepton analysis:** optimised semi-leptonic decay vertex reconstruction and an improved production flavour tag,
- **$D_s$ –lepton correlation analysis:** proper time resolution now extracted event-by-event.

These new results, when combined with the results of other approaches, give the following, final, results from DELPHI concerning  $B_s^0$  oscillations:

$$\Delta m_s > 8.5 \text{ ps}^{-1} @ 95\% \text{ C.L.}$$

$$\text{Sensitivity, } \Delta m_s = 12.0 \text{ ps}^{-1} @ 95\% \text{ C.L.}$$

### 4 A study of $B^{**}$ states

Heavy Quark Theory predicts that the  $B^{**}$  states should exist in the form of two doublets:  $J^P = 0^+, 1^+$  which decay in a relative S-wave and hence have broad strong interaction widths and  $J^P = 1^+, 2^+$  which have narrow widths because they decay in a relative D-wave. More detailed predictions of  $B^{**}$  properties from theory are numerous but suffer from being highly model dependent and so progress in this field is largely experimentally driven. The motivation for analyses in this area is increased by a review of the current experimental status: Knowledge of the broad  $B^{**}$  states is currently non-existent and results on  $B_{u,d}^{**}$  narrow states from the LEP experiments

and CDF [4] fail to agree on the production rate, probably because of uncertainties in estimating the background contribution. For the case of  $B_s^{**}$ , one measurement from OPAL [5] exists which needs confirmation.

What follows is a brief update of on-going DELPHI studies into  $B_{u,d}^{**}$  and  $B_s^{**}$  states and full details can be found in [6].

#### 4.1 $B_{u,d}^{**}$ analyses

Searches were made in the channels,  $B_u^{**} \rightarrow B^0 \pi^+$  and  $B_d^{**} \rightarrow B^+ \pi^-$  with two different approaches:

- **High Efficiency Approach (HEA):** minimises input from the simulation by fitting an analytical parameterisation of the background to the data.
- **High Purity Approach (HPA):** targets the best possible signal to background ratio by using neural network techniques for  $B^{**}$  signal enhancement.

Features that are common to both approaches include:

- an inclusive reconstruction of  $B^+, B^0$ ,
- identification of the  $B^{**}$  decay pion from the background of tracks originating from the fragmentation process,
- dividing the data into ‘right’- and ‘wrong-sign’ samples, defined by the charge correlation that exists between the  $B^{**}$  decay pion and the  $b$ -quark in the parent  $B^{**}$  state,
- reconstruction of the  $Q$  value for the decay defined as,  $Q = m(B^{(*)}\pi) - m(B^{(*)}) - m(\pi)$ ,
- fitting the  $Q$ -value distribution with the sum of a Gaussian and a Breit-Wigner component plus a background parameterisation.

Fits are made simultaneously to the right- and wrong-sign distributions with the  $B_u^{**}$  and  $B_d^{**}$  samples treated as one in the HEA but kept separate in the HPA. The results of the fits are summarised in Table 1 where the first quoted error is statistical and the second systematic. Inclusion of a Breit-Wigner component to the signal fit function was found to significantly improve the fit quality in both analyses. The fit from the HPA for the  $B_d^{**}$  right and wrong-sign samples is shown in Fig. 2. The expectation is that the narrow  $B^{**}$  states produce three narrow peaks in  $Q$ -value resulting from: (a) a hyperfine mass splitting between the  $B_1$  and  $B_2^*$  states of about 12 MeV and (b) the  $B_2^*$  can decay to both  $B\pi$  and  $B^*\pi$  final states separated in  $Q$ -value by the 46 MeV carried away by the  $B^*$  decay photon. Simulation studies show that these features are not resolvable within the experimental resolution attainable and both analyses find Gaussian peaks with widths compatible with the resolution. It is therefore reasonable to interpret the Gaussian rates quoted in Table 1 as narrow  $B^{**}$  rates. For the broad  $B^{**}$  states the situation is less clear. Interpreting the Breit-Wigner component as a broad state or combination of states would give evidence for broad  $B^{**}$  states at the  $2.5 - 3\sigma$  level as estimated by the High Efficiency Approach and would verify the spin-orbit inversion prediction for the narrow/broad mass hier-

**Table 1.** Results from the two DELPHI  $B_{u,d}^{**}$  analyses. The sub-script ‘Gauss’ and ‘BW’ refer to parameters from the Gaussian and Breit-Wigner components of the fit function. Measured rates have been scaled by a factor 1.5 to account for the unmeasured  $B^{**} \rightarrow B^{0(*)}\pi^0$  decay channel.

	High Efficiency Approach	High Purity Approach
$\chi^2/\text{d.o.f}$	0.9	1.0
$\langle Q_{\text{Gauss}} \rangle$	$292 \pm 3 \pm 12$ MeV	$286 \pm 3 \pm 3$ MeV
$\sigma(Q_{\text{Gauss}})$	$45 \pm 4 \pm 4$ MeV	$B_u^{**} : 57 \pm 6 \pm 4$ MeV $B_d^{**} : 46 \pm 5 \pm 3$ MeV
$\text{Rate}_{\text{Gauss}}$	$0.122 \pm 0.014 \pm 0.018$	$0.143 \pm 0.014 \pm 0.018$
$\langle Q_{\text{BW}} \rangle$	$517 \pm 18 \pm 30$ MeV	$510 \pm 20 \pm 20$ MeV
$\Gamma(Q_{\text{BW}})$	$295 \pm 47 \pm 50$ MeV	$380 \pm 130 \pm 210$ MeV
$\text{Rate}_{\text{Gauss+BW}}$	$0.196 \pm 0.029 \pm 0.030$	$0.199 \pm 0.029 \pm 0.033$
$\text{Ratio}(\frac{\text{BW}}{G})$	$0.60 \pm 0.24 \pm 0.20$	$0.39 \pm 0.17 \pm 0.19$

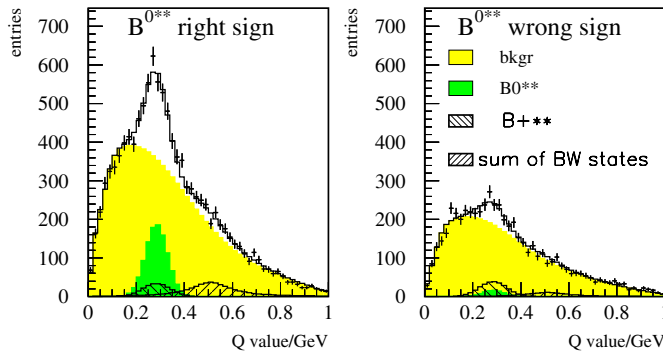


**Fig. 2.** The points show the  $Q$ -distribution of the right and wrong-sign samples in data and the solid histogram the result of the fit. The composition of the fit function components are also displayed.

archy. Recent results from the charm sector however suggest that broad states are perhaps more likely to sit lower in mass than the narrow states and studies to investigate this possibility are underway.

## 4.2 Reconstructing the $B_s^{**}$

An analysis to reconstruct  $B_s^{**}$  states has been made within the framework of the HPA in the channel  $B_s^{**} \rightarrow B^+ K^-$ . The analysis proceeds in an analogous way to the  $B_{u,d}^{**}$  search with the replacement of the decay pion with a kaon. The kaon is isolated by a  $B_s^{**}$  neural network trained to identify  $B_s^{**}$  decay kaons from the fragmentation background and makes extensive use of the excellent particle identification capability of the DELPHI detector.

The low statistics expected for  $B_s^{**}$  production (i.e.  $\text{BR}(b \rightarrow B_s^{**}) < 4\%$  before acceptance) means that the use of reliable constraints from the simulation are necessary:

- the narrow  $B_s^{**}$   $Q$ -value shape is parameterised as a double Gaussian based on the experimental resolution estimated in simulation from passing a delta function

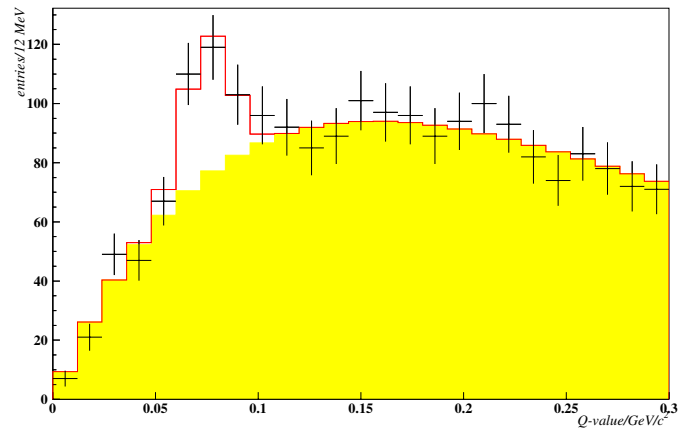


**Fig. 3.** An example of a fit (histogram) to the  $Q$ -value distribution in the data (points) for a  $B_s^{**}$ -enhanced sample. The shape of the background component is overlaid.

centered at 80 MeV  $Q$ -value through the reconstruction chain,

- the background shape as seen in simulation is assumed with a slope correction function applied and the parameters left free in the fit.

There is no sensitivity to broad  $B_s^{**}$  states and the fit function absorbs them into the definition of the background.

By varying the working point cuts for  $B_s^{**}$  purity, decay kaon purity and  $Q$ -value resolution,  $B_s^{**}$  samples were formed and fitted over a range of working points. Figure 3 shows an example of such a fit at a typical working point. A clear signal can be seen which has a significance of  $> 3\sigma$  to not be compatible with being a fluctuation of the background shape. The resulting mean  $Q$ -value and rate for the signal is,

$$\begin{aligned} \langle Q \rangle &= 76.3 \pm 3.2(\text{stat.}) \pm 4.7(\text{syst.}) \text{ MeV} \\ \text{Rate} &= 0.010 \pm 0.002(\text{stat.}) \pm 0.003(\text{syst.}) \end{aligned}$$

where the rate has been scaled by a factor two to account for the unmeasured  $B_s^{**} \rightarrow B^{0(*)}K^0$  channel.

## References

1. C. Weiser, *A measurement of the branching fractions of the b-quark into charged and neutral b-hadrons*, contributed paper (# 329) to EPS 2003 (Aachen)
2. ALEPH, CDF, DELPHI, L3, OPAL, SLD, CERN-EP/2001-050
3. DELPHI Collab.: *Search for  $B_s^0 - \bar{B}_s^0$  Oscillations in DELPHI*, contributed paper (# 378) to EPS 2003 (Aachen)
4. DELPHI Collab.: Phys. Lett. B **345**, 598 (1995); ALEPH Collab.: Z. Phys. C **69**, 393 (1996); CDF Collab.: Phys. Rev. D **64**, 072002 (2001); OPAL Collab.: Z. Phys. C **66**, 19 (1995); L3 Collab.: Phys. Lett. B **465**, 323 (1999)
5. OPAL Collab.: Z. Phys. C **66**, 19 (1995)
6. Z. Albrecht et. al.: *A Study of Excited b-hadron States with the DELPHI Detector at LEP*, contributed paper (# 328) to EPS 2003 (Aachen)